

## ON FRACTAL PATTERNS FOR MULTI-WING HYPERCHAOTIC ATTRACTORS WITH A MIRROR SYMMETRICAL STRUCTURE

EMILE F. DOUNGMO GOUFO

**Abstract.** Hyperchaos remains one of the most complex behaviors in the bifurcation mechanisms and so far, only few hyperchaotic dynamics have been identified experimentally. The construction and design of complex models able to generate hyperchaotic attractors with wings on many rows and columns have become a source of interest for many fractal & chaos theorists, applied physicists and engineers. In this paper, we make use of a simple method, that consists on combining the fractal and fractional operator with Lü system, in order to generate second class hyperchaotic attractors with wings on many rows and columns. Such a combination yields a modified initial value problem, that is solved both analytically and numerically. We then implement the proposed scheme to perform some graphical representations showing the second class types of attractors in the form  $n \times m$ -wings, ( $n, m \in \mathbb{N}$ ), which appear to be hyperchaotic and exhibit a mirror symmetrical structure. The graphical simulations also depict a process where the lower and upper parts of the second class hyperchaotic attractors are seen to be moving away from the mirror symmetrical junction due to the parameter's impact of the fractal-fractional operator.

### 1. Introductory remarks and preliminaries

The concept of hyperchaotic behavior was introduced decades ago when the German author Rössler proposed its equation for hyperchaos [25] and since then, the interest for such a complex dynamics has never stopped growing among the researchers. Hence we have seen the the development of many other systems related to the generation of chaotic and hyperchaotic behaviors such as Lorenz system, Chua system, Sprott system, Rössler system and hyperchaotic Lorenz system, proto-Lorenz system and proto-Lü system [9, 6, 21, 7, 10, 19, 11, 22, 20, 28]. In many instances, hyperchaotic attactors have been generated by introducing into the model, additional terms such as linear or nonlinear quadratic controllers [6, 21, 29, 30]. Second class hyperchaotic attactors are generated using a similar approach. We propose another method here applicable to hyperchaotic models

---

2010 *Mathematics Subject Classification.* 34D45; 37D45; 26A33; 65P20; 65P30.

*Key words and phrases.* Hyperchaotic attractors, multiwing systems, numerical methods, fractal-fractional structure.

and suitable for the generation second class hyperchaotic attractors with wings on many rows and columns. Hence, consider the following modified hyperchaotic Lü system [29, 30]

$$\begin{cases} \frac{dx(t)}{dt} = -\delta_{11}x + \delta_{12}y + \delta_{13}u, \\ \frac{dy(t)}{dt} = -\delta_{21}xz + \delta_{22}y, \\ \frac{dz(t)}{dt} = \delta_{31}y^2 + \delta_{32}z, \\ \frac{du(t)}{dt} = \delta_{41}xz + \delta_{42}u. \end{cases} \tag{1.1}$$

where the coefficients are real numbers. The authors in [29, 30] show that is possible to modify such a hyperchaotic system to get a different system which takes the form of an attractor with  $n + m$  number of wings and denoted as  $n \times m$ -wings, with  $n, m \in \mathbb{N}$ . The resulting attractor is also expected to be hyperchaotic and to express it, we can insert into (1.1) an additional function denoted by  $\mathbf{F}$ , dependent on the variable  $y$  so as to have

$$\begin{cases} \frac{dx(t)}{dt} = -\delta_{11}x + \delta_{12}y + \delta_{13}u, \\ \frac{dy(t)}{dt} = -\delta_{21}xz + \delta_{22}y, \\ \frac{dz(t)}{dt} = \mathbf{F}(y) - \delta_{32}z, \\ \frac{du(t)}{dt} = \delta_{41}xz + \delta_{42}u. \end{cases} \tag{1.2}$$

The function  $\mathbf{F}(y)$  is called a duality-symmetric multi-segment quadratic function expressed as

$$\mathbf{F}(y) = A_0y^2 + \sum_{k=1}^{\mathbf{T}} A_k \left( \text{sgn}(y + \tilde{A}_k) - \text{sgn}(y - \tilde{A}_k) - 2 \right) \tag{1.3}$$

with  $k = 1, 2, \dots, \mathbf{T}$  where  $\mathbb{N} \ni \mathbf{T} \geq 1$ . The coefficients  $A_k$ ,  $k = 0, 1, 2, \dots, \mathbf{T}$  and  $\tilde{A}_k$  reads as

$$\begin{cases} A_0 = \rho, \\ A_k = \frac{\alpha}{\rho_k}, \\ \tilde{A}_k = \frac{\alpha}{2\rho}(k + 1). \end{cases} \tag{1.4}$$

Now, we can make use of the system (1.2) to express a hyperchaotic model with mirror symmetry conversion system that reads as

$$\begin{cases} \frac{dx}{dt}(t) = -\delta_{11}x + \delta_{12}y + \delta_{13}u, \\ \frac{dy}{dt}(t) = -\delta_{21}x \times [\text{sgn}(z - \tilde{z}) \times (z - \tilde{z}) - \mathbf{G}(z)] + \delta_{22}y, \\ \frac{dz}{dt}(t) = \text{sgn}(z - \tilde{z}) \times \mathbf{F}(y) - \delta_{32}[(z - \tilde{z}) + \text{sgn}(z - \tilde{z}) \times \mathbf{G}(z)], \\ \frac{du}{dt}(t) = \delta_{41}x \times [\text{sgn}(z - \tilde{z}) \times (z - \tilde{z}) - \mathbf{G}(z)] + \delta_{42}u. \end{cases} \tag{1.5}$$

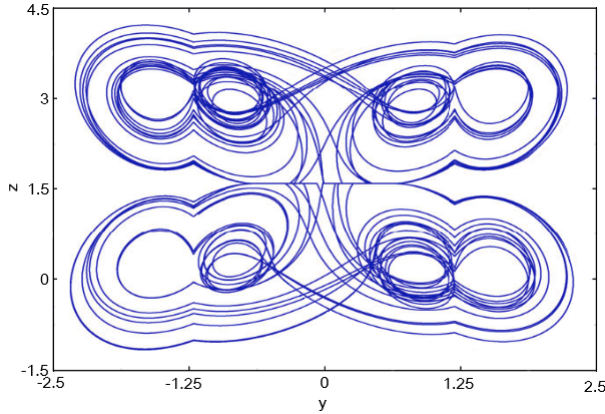


FIGURE 1. Numerical representation of the system (1.5) showing a second class of hyperchaotic attractor (with a mirror junction) of type  $4 \times 2$ -wings in the plan  $yz$ , when  $\mathbf{M} = 0$ ,  $\mathbf{G}(z) = 0$ . The parameter values used read as  $\mathbf{T} = 1$ ,  $\rho = 17.9$ ,  $\rho_1 = 1.7$ ,  $\rho_2 = 1.45$   $\alpha = 18$  and then,  $A_0 = 17.9$ ,  $A_1 = 10.59$ ,  $A_2 = 12.41$ ,  $\tilde{A}_1 = 1.0056$ ,  $\tilde{A}_2 = 1.5084$ .

The function  $\mathbf{F}$  has already been defined in (1.3) and the  $z$  dependent function  $\mathbf{G}$  represents the mirror symmetry conversion function and expressed by

$$\mathbf{G}(z) = \sum_{k=1}^{\mathbf{M}} (\pm\Phi \cdot (1 \pm \text{sgn}(\text{sgn}(z - \tilde{z}) \times (z - \tilde{z}) - (z_k - \tilde{z}))))). \quad (1.6)$$

This model is able to generate the so-called second class of hyperchaotic attractor with  $(2\mathbf{T} + 2) + (2\mathbf{M} + 2)$  number of wings (denoted in form  $(2\mathbf{T} + 2) \times (2\mathbf{M} + 2)$ -wing). Hence, taking  $\mathbf{M} = 0$ ,  $\mathbf{G}(z) = 0$  and for the parameter values  $\mathbf{T} = 1$  and  $\mathbf{T} = 2$ , we respectively obtain the numerical representations of the system (1.5) depicting a second class of hyperchaotic attractor of type  $4 \times 2$ -wings in the plan  $yz$  as shown in Fig. 1 and of type  $6 \times 2$ -wings as shown in Fig. 2. The other parameters used are  $\rho = 17.9$ ,  $\rho_1 = 1.7$ ,  $\rho_2 = 1.45$   $\alpha = 18$ . Using (1.4) we obtain  $A_0 = 17.9$ ,  $A_1 = 10.59$ ,  $A_2 = 12.41$ ,  $\tilde{A}_1 = 1.0056$ ,  $\tilde{A}_2 = 1.5084$ . Now considering  $\mathbf{T} = 7$ ,  $\mathbf{M} = 1$ , and taking  $\mathbf{G}(z) \neq 0$  so that  $\Phi = 1.05$ ,  $\tilde{z} = -2.5$ ,  $z_1 = 4$  then  $\mathbf{G}(z)$  becomes

$$\mathbf{G}(z) = \Phi(1 + \text{sgn}(\text{sgn}(z - \tilde{z}) \times (z - \tilde{z}) - (z_1 - \tilde{z}))).$$

With these values, we obtain the numerical representation of the second class of hyperchaotic attractor of type  $16 \times 4$ -wings in the plan  $yz$  as depicted in Fig. 3.

- Remark 1.1.*
- (1) Both attractors are shown to have incorporated the mirror symmetry conversion system as the upper part of the attractor seems to be the mirror reflection of the lower part
  - (2) The circuit diagram used to establish such second class of  $n \times m$ -wing hyperchaotic models with a mirror system is given by Fig. 4.

The question we ask now is whether there exist other alternative methods, maybe less complicated, and that can generate similar hyperchaotic models.

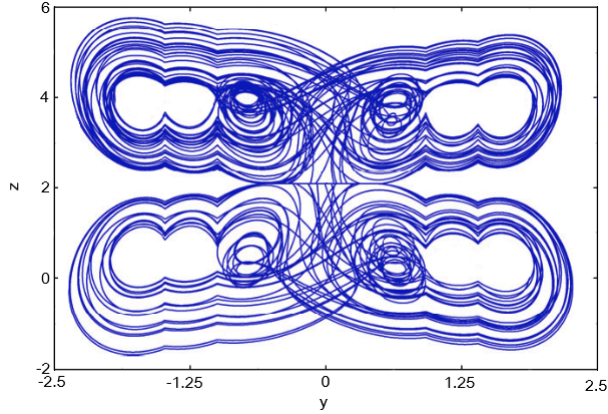


FIGURE 2. Numerical representation of the system (1.5) showing a second class of hyperchaotic attractor (with a mirror junction) of type  $6 \times 2$ -wings in the plan  $yz$ , when  $\mathbf{M} = 0$ ,  $\mathbf{G}(z) = 0$ . The parameter values used read as  $\mathbf{T} = 2$ ,  $\rho = 17.9$ ,  $\rho_1 = 1.7$ ,  $\rho_2 = 1.45$ ,  $\alpha = 18$  and then,  $A_0 = 17.9$ ,  $A_1 = 10.59$ ,  $A_2 = 12.41$ ,  $\tilde{A}_1 = 1.0056$ ,  $\tilde{A}_2 = 1.5084$ .

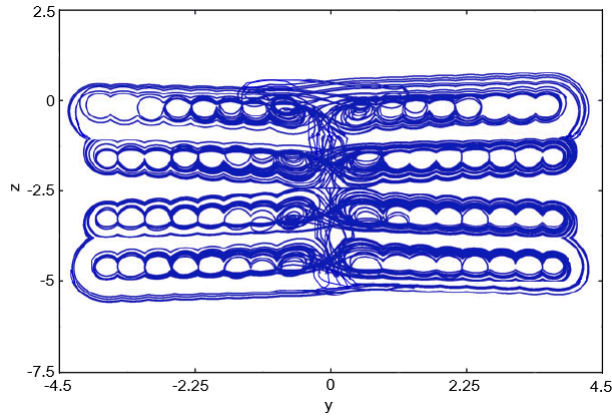


FIGURE 3. Numerical representation of the system (1.5) showing a second class of hyperchaotic attractor (with a mirror junction) of type  $16 \times 4$ -wings in the plan  $yz$ , when  $\mathbf{M} = 1$ , and taking  $\mathbf{G}(z) \neq 0$  with  $\mathbf{G}(z) = \Phi(1 + \text{sgn}(\text{sgn}(z - \tilde{z}) \times (z - \tilde{z}) - (z_1 - \tilde{z})))$  and for  $\mathbf{T} = 7$ , so that  $\Phi = 1.05$ ,  $\tilde{z} = -2.5$ ,  $z_1 = 4$ . The other parameter values used are  $\rho = 17.9$ ,  $\rho_1 = 1.7$ ,  $\rho_2 = 1.45$ ,  $\rho_3 = 1$ ,  $\rho_4 = 0.8$ ,  $\rho_5 = 0.65$ ,  $\rho_6 = 0.57$ ,  $\rho_7 = 0.55$ ,  $\alpha = 18$ ,  $A_0 = 17.9$ ,  $A_1 = 10.59$ ,  $A_2 = 12.41$ ,  $A_3 = 18$ ,  $A_4 = 22.5$ ,  $A_5 = 27.69$ ,  $A_6 = 31.58$ ,  $A_7 = 32.73$ ,  $\tilde{A}_1 = 1.0056$ ,  $\tilde{A}_2 = 1.5084$ ,  $\tilde{A}_3 = 2.0112$ ,  $\tilde{A}_4 = 2.514$ ,  $\tilde{A}_5 = 3.0168$ ,  $\tilde{A}_6 = 3.5196$ ,  $\tilde{A}_7 = 4.0223$ .

## 2. Generation of the fractal patterns for the multi-wing hyperchaotic attractors with a mirror symmetrical structure

Recall that dynamical systems which display a fractal structure have been intensively analysed and simulated in the last years by a growing number of researchers [14, 24, 23, 16, 12, 4, 13, 5] where they managed to recreate and generate chaotic bifurcation dynamics using different methods involving, in one way or another, fractal design. In this section, we show how to use the fractal

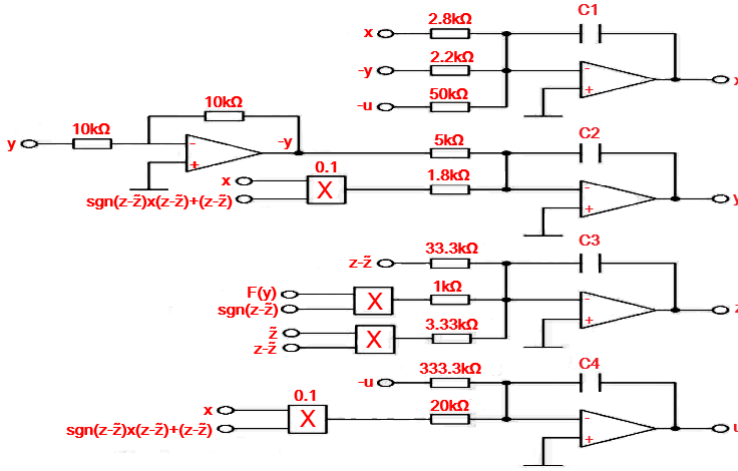


FIGURE 4. Circuit diagram used to establish such second class of  $n \times m$ -wing hyperchaotic models with a mirror system,  $(n, m \in \mathbb{N})$ .

and fractional processes to generate second class of hyperchaotic attractors of type  $n \times m$ -wing. For that, we need to state the following definitions

**Definition 2.1.** • Let  $t > 0$  and consider the subspace  $E \subseteq \mathbb{R}^+$ , in which we define  $\varphi : E \rightarrow \mathbb{R}, t \mapsto \varphi(t)$ . Let  $(a_1, a_2) \subset E$  an open interval  $(a_1, a_2 \in \mathbb{R}^+)$ . We assume that  $\varphi$  fractal-differentiable on  $(a_1, a_2)$  at the order  $q \in (0, 1)$ . Then, we define the fractal-fractional derivative of the function  $\varphi$  with order  $q$  in Riemann-Liouville sense, with power law kernel as

$${}^{frp}D_t^q \varphi(t) = \frac{1}{\Gamma(1-q)} \frac{\partial}{\partial t^q} \int_0^t \varphi(\omega) (t-\omega)^{-q} d\omega, \tag{2.1}$$

where  $\frac{\partial}{\partial t^q} \varphi$  is defined as

$$\frac{\partial}{\partial t^q} \varphi(\xi) = \lim_{t \rightarrow \xi} \frac{\varphi(t) - \varphi(\xi)}{t^q - \xi^q}$$

- Its generalized version is

$${}^{frp}D_t^{q,\iota} \varphi(t) = \frac{1}{\Gamma(1-q)} \frac{\partial^\iota}{\partial t^q} \int_0^t \varphi(\omega) (t-\omega)^{-q} d\omega, \tag{2.2}$$

with  $\iota > 0$  and  $\frac{\partial^\iota}{\partial t^q} \varphi$  given by

$$\frac{\partial^\iota}{\partial t^q} \varphi(\xi) = \lim_{t \rightarrow t_0} \frac{\varphi^\iota(t) - \varphi^\iota(t_0)}{t^q - \xi^q}.$$

- We define the fractal-fractional derivative of the function  $\varphi$  with order  $q$  in Caputo sense, with power law kernel as

$${}^{fcp}D_t^q \varphi(t) = \frac{1}{\Gamma(1-q)} \int_0^t \frac{\partial}{\partial \omega^q} \varphi(\omega) (t-\omega)^{-q} d\omega, \tag{2.3}$$

- Its generalized version is

$${}^{fcp}D_t^{q,\iota}\varphi(t) = \frac{1}{\Gamma(1-q)} \int_0^t \frac{\partial^\iota}{\partial\omega^q} \varphi(\omega) (t-\omega)^{-q} d\omega, \tag{2.4}$$

We refer to the Caputo sense fractal-fractional derivative with power law kernel  ${}^{fcp}D_t^q$  given in (2.3) of Definition 2.1 in order to generate second class hyperchaotic attractors. To this end, we will need its corresponding anti-derivative of order  $q$ , that is

$${}^{fcp}I_t^q\varphi(t) = \frac{q}{\Gamma(q)} \int_0^t \chi^{-q}\varphi(\chi)(t-\chi)^{q-1}d\chi, \quad t > 0. \tag{2.5}$$

Knowing these preliminary definitions, the system (1.5) can be modified to become a fractional-fractal model taking the expression

$$\begin{cases} {}^{fcp}D_t^q x(t) = -\delta_{11}x + \delta_{12}y + \delta_{13}u, \\ {}^{fcp}D_t^q y(t) = -\delta_{21}x \times [\text{sgn}(z - \tilde{z}) \times (z - \tilde{z}) - \mathbf{G}(z)] + \delta_{22}y, \\ {}^{fcp}D_t^q z(t) = \text{sgn}(z - \tilde{z}) \times \mathbf{F}(y) - \delta_{32}[(z - \tilde{z}) + \text{sgn}(z - \tilde{z}) \times \mathbf{G}(z)], \\ {}^{fcp}D_t^q u(t) = \delta_{41}x \times [\text{sgn}(z - \tilde{z}) \times (z - \tilde{z}) - \mathbf{G}(z)] + \delta_{42}u. \end{cases} \tag{2.6}$$

To solve this model, it is necessary to consider its initial conditions

$$x(0) = \bar{x}(x), \quad y(0) = \bar{y}(y), \quad z(0) = \bar{z}(z), \quad u(0) = \bar{u}(u). \tag{2.7}$$

The transformation the initial value problem (2.6)-(2.7) into a compact problem is possible via the use of state vectors

$$\boldsymbol{\eta}(t) = (x(t), y(t), z(t), u(t))$$

$$\boldsymbol{\eta}_0(x, y, z) = \boldsymbol{\eta}(0) = (x(0), y(0), z(0), u(0)) = (\bar{x}, \bar{y}, \bar{z}, \bar{u}).$$

Moreover, we also define

the matrix  $\mathbb{O}$  expressed by

$$\mathbb{O}(\boldsymbol{\eta}(t), t) = \mathbb{O}(x(t), y(t), z(t), u(t), t) =$$

$$(\mathbb{O}_1(\boldsymbol{\eta}(t), t), \mathbb{O}_2(\boldsymbol{\eta}(t), t), \mathbb{O}_3(\boldsymbol{\eta}(t), t), \mathbb{O}_4(\boldsymbol{\eta}(t), t)),$$

which is then assumed to depend on  $x, y, z, u$  so as to have:

$$\begin{cases} \mathbb{O}_1(\boldsymbol{\eta}(t), t) = \mathbb{O}_1(x(t), y(t), z(t), u(t), t) = -\delta_{11}x + \delta_{12}y + \delta_{13}u, \\ \mathbb{O}_2(\boldsymbol{\eta}(t), t) = \mathbb{O}_2(x(t), y(t), z(t), u(t), t) = \\ \quad -\delta_{21}x \times [\text{sgn}(z - \tilde{z}) \times (z - \tilde{z}) - \mathbf{G}(z)] + \delta_{22}y, \\ \mathbb{O}_3(\boldsymbol{\eta}(t), t) = \mathbb{O}_3(x(t), y(t), z(t), u(t), t) = \\ \quad \text{sgn}(z - \tilde{z}) \times \mathbf{F}(y) - \delta_{32}[(z - \tilde{z}) + \text{sgn}(z - \tilde{z}) \times \mathbf{G}(z)], \\ \mathbb{O}_4(\boldsymbol{\eta}(t), t) = \mathbb{O}_4(x(t), y(t), z(t), u(t), t) = \delta_{41}x \times [\text{sgn}(z - \tilde{z}) \times (z - \tilde{z}) - \mathbf{G}(z)] \\ \quad + \delta_{42}u \end{cases}$$

or equivalently

$$\left\{ \begin{array}{l} \mathbb{O}_1(\boldsymbol{\eta}(t), t) = \mathbb{O}_1(x(t), y(t), z(t), u(t), t) = -\delta_{11}x + \delta_{12}y + \delta_{13}u, \\ \mathbb{O}_2(\boldsymbol{\eta}(t), t) = \mathbb{O}_2(x(t), y(t), z(t), u(t), t) = \\ \quad -\delta_{21}x \times [\text{sgn}(z - \tilde{z}) \times (z - \tilde{z}) - \mathbf{G}(z)] + \delta_{22}y, \\ \mathbb{O}_3(\boldsymbol{\eta}(t), t) = \mathbb{O}_3(x(t), y(t), z(t), u(t), t) = \\ \quad \text{sgn}(z - \tilde{z}) \times \left[ A_0 y^2 + \sum_{k=1}^{\mathbf{T}} A_k \left( \text{sgn}(y + \tilde{A}_k) - \text{sgn}(y - \tilde{A}_k) - 2 \right) \right] - \\ \quad \delta_{32}[(z - \tilde{z}) + \text{sgn}(z - \tilde{z}) \times \mathbf{G}(z)], \\ \mathbb{O}_4(\boldsymbol{\eta}(t), t) = \mathbb{O}_3(x(t), y(t), z(t), u(t), t) = \delta_{41}x \times [\text{sgn}(z - \tilde{z}) \times (z - \tilde{z}) - \mathbf{G}(z)] \\ + \delta_{42}u \end{array} \right.$$

Thus, the resulting compact system obtained from (2.6) takes the form

$${}^{fcp}D_t^q \boldsymbol{\eta}(t) = \mathbb{O}(\boldsymbol{\eta}(t), t)$$

equivalently,

$$\begin{aligned} {}^{fcp}D_t^q x(t) &= \mathbb{O}_1(\boldsymbol{\eta}(t), t) \\ {}^{fcp}D_t^q y(t) &= \mathbb{O}_2(\boldsymbol{\eta}(t), t) \\ {}^{fcp}D_t^q z(t) &= \mathbb{O}_3(\boldsymbol{\eta}(t), t) \\ {}^{fcp}D_t^q u(t) &= \mathbb{O}_4(\boldsymbol{\eta}(t), t), \end{aligned} \quad (2.8)$$

with initial conditions

$$x(0) = \bar{x}(x), \quad y(0) = \bar{y}(y), \quad z(0) = \bar{z}(z), \quad u(0) = \bar{u}(u).$$

With reference to the numerical method of Haar wavelets as defined, developed and described in [2, 18], we can approximate the main function  $\boldsymbol{\eta}$  using the Haar orthonormal basis functions  $\phi_{k,j}$  so as to get

$$\boldsymbol{\eta}(t) \approx \boldsymbol{\eta}_\mu(t) = \sum_{k=1}^{\mathbf{m}} \sum_{j=0}^{\mu-1} \phi_{k,j} W_{k,j}(t) \quad (2.9)$$

with  $\mu \in \{2^i : i = 0, 1, 2, \dots\}$ ,

$$\phi_{k,j} = \langle \boldsymbol{\eta}, W_{k,j} \rangle = \int_0^\infty \boldsymbol{\eta}(t) W_{k,j}(t) dt.$$

The quantity  $W_{k,j}$  is referred to as Haar function and reads as

$$W_{k,j}(t) = W_j(t - k + 1) \quad k = 1, 2, \dots, \mathbf{m} \quad \text{and} \quad j = 0, 1, 2, \dots \quad (2.10)$$

where

$$W_j(t) = \begin{cases} 2^{\frac{j}{2}} \mathbb{B}(2^j t - \mu), & \text{for } j = 1, 2, \dots; \\ 1, & \text{for } j = 0, \end{cases} \quad (2.11)$$

and

$$\mathbb{B}(t) = \begin{cases} 1, & \text{when } 0 \leq t < 1/2; \\ -1, & \text{for } 1/2 \leq t < 1; \\ 0, & \text{everywhere else.} \end{cases} \quad (2.12)$$

Recall the main property that has helped us reaching this results which is: Every number  $j \in \{0, 1, 2, 3, \dots\}$  can be expressed using the power form  $j = 2^i + \mu$  for  $i = 0, 1, 2, \dots$  and  $\mu = 0, 1, 2, \dots, 2^i - 1$ .

To further complete our analysis, it is important to use the fact that (2.9) can explicitly be transformed in

$$\eta(t) \approx \eta_\mu(t) = \mathbf{B}_{\mathbf{m}\mu \times 1}^T \mathbf{E}_{\mathbf{m}\mu \times 1} \tag{2.13}$$

with the vector  $\mathbf{B}_{\mathbf{m}\mu \times 1}$  reading as

$$\mathbf{B}_{\mathbf{m}\mu \times 1} = (\phi_{1,0}, \dots, \phi_{1,\mu-1}, \phi_{2,0}, \dots, \phi_{2,\mu-1}, \dots, \phi_{\mathbf{m},0}, \dots, \phi_{\mathbf{m},\mu-1},)$$

and the transpose  $^T \mathbf{E}_{\mathbf{m}\mu \times 1}$  of the vector  $\mathbf{E}_{\mathbf{m}\mu \times 1}$  given by

$$\mathbf{E}_{\mathbf{m}\mu \times 1} = (W_{1,0}, \dots, W_{1,\mu-1}, W_{2,0}, \dots, W_{2,\mu-1}, \dots, W_{\mathbf{m},0}, \dots, W_{\mathbf{m},\mu-1},)$$

Using the Caputo sense fractal-fractional operator  ${}^{fcp}D_t^q$  defined earlier and resulting model (2.8) on which  ${}^{fcp}D_t^q$  is applied, we obtain for the whole system approximation scheme

$$\begin{aligned} {}^{fcp}D_t^q x(t) &= \mathbb{O}_1(\eta(t), t) \approx {}^{fcp}D_t^q x_\mu(t) = {}^T \mathbf{B}_{\mathbf{m}\mu \times 1}^1 \mathbf{E}_{\mathbf{m}\mu \times 1} \\ {}^{fcp}D_t^q y(t) &= \mathbb{O}_2(\eta(t), t) \approx {}^{fcp}D_t^q y_\mu(t) = {}^T \mathbf{B}_{\mathbf{m}\mu \times 1}^2 \mathbf{E}_{\mathbf{m}\mu \times 1} \\ {}^{fcp}D_t^q z(t) &= \mathbb{O}_3(\eta(t), t) \approx {}^{fcp}D_t^q z_\mu(t) = {}^T \mathbf{B}_{\mathbf{m}\mu \times 1}^3 \mathbf{E}_{\mathbf{m}\mu \times 1} \\ {}^{fcp}D_t^q u(t) &= \mathbb{O}_4(\eta(t), t) \approx {}^{fcp}D_t^q u_\mu(t) = {}^T \mathbf{B}_{\mathbf{m}\mu \times 1}^4 \mathbf{E}_{\mathbf{m}\mu \times 1}. \end{aligned} \tag{2.14}$$

Now the antiderivative (2.5) is applied on both sides of this system (2.14) to have

$$\begin{aligned} x(t) - \bar{x} &\approx {}^{fcp}D_t^q x_\mu(t) = {}^T \mathbf{B}_{\mathbf{m}\mu \times 1}^1 \Theta_{\mathbf{m}\mu \times \mathbf{m}\mu}^q \mathbf{E}_{\mathbf{m}\mu \times 1} \\ y(t) - \bar{y} &\approx {}^{fcp}D_t^q y_\mu(t) = {}^T \mathbf{B}_{\mathbf{m}\mu \times 1}^2 \Theta_{\mathbf{m}\mu \times \mathbf{m}\mu}^q \mathbf{E}_{\mathbf{m}\mu \times 1} \\ z(t) - \bar{z} &\approx {}^{fcp}D_t^q z_\mu(t) = {}^T \mathbf{B}_{\mathbf{m}\mu \times 1}^3 \Theta_{\mathbf{m}\mu \times \mathbf{m}\mu}^q \mathbf{E}_{\mathbf{m}\mu \times 1} \\ u(t) - \bar{u} &\approx {}^{fcp}D_t^q u_\mu(t) = {}^T \mathbf{B}_{\mathbf{m}\mu \times 1}^4 \Theta_{\mathbf{m}\mu \times \mathbf{m}\mu}^q \mathbf{E}_{\mathbf{m}\mu \times 1}, \end{aligned} \tag{2.15}$$

that also take the equivalent form

$$\begin{aligned} x(t) &\approx x_\mu(t) = {}^T \mathbf{B}_{\mathbf{m}\mu \times 1}^1 \Theta_{\mathbf{m}\mu \times \mathbf{m}\mu}^q \mathbf{E}_{\mathbf{m}\mu \times 1} + \bar{x} \\ y(t) &\approx y_\mu(t) = {}^T \mathbf{B}_{\mathbf{m}\mu \times 1}^2 \Theta_{\mathbf{m}\mu \times \mathbf{m}\mu}^q \mathbf{E}_{\mathbf{m}\mu \times 1} + \bar{y} \\ z(t) &\approx z_\mu(t) = {}^T \mathbf{B}_{\mathbf{m}\mu \times 1}^3 \Theta_{\mathbf{m}\mu \times \mathbf{m}\mu}^q \mathbf{E}_{\mathbf{m}\mu \times 1} + \bar{z} \\ u(t) &\approx u_\mu(t) = {}^T \mathbf{B}_{\mathbf{m}\mu \times 1}^4 \Theta_{\mathbf{m}\mu \times \mathbf{m}\mu}^q \mathbf{E}_{\mathbf{m}\mu \times 1} + \bar{z}, \end{aligned} \tag{2.16}$$

where the quantity  $\Theta_{\mathbf{m}\mu \times \mathbf{m}\mu}^q$  is Haar fractional operational matrix [2, 8]. We finalize the solvability of the initial value problem (2.6)-(2.7) by making use of the collocation points approach of the Galerkin method. Hence, it allows the substitution of the two systems (2.14) and (2.16) into the model (2.6), which

leads to the generation of the residual errors expressed as

$$\begin{aligned}
\vartheta_1(\tau^1, \tau^2, \tau^3, t) &= {}^T \mathbf{B}_{\mathbf{m}\mu \times 1}^1 \mathbf{E}_{\mathbf{m}\mu \times 1} - \mathbb{O}_1 \left( {}^T \mathbf{B}_{\mathbf{m}\mu \times 1}^1 \Theta_{\mathbf{m}\mu \times \mathbf{m}\mu}^q \mathbf{E}_{\mathbf{m}\mu \times 1}, \right. \\
&\quad \left. {}^T \mathbf{B}_{\mathbf{m}\mu \times 1}^2 \Theta_{\mathbf{m}\mu \times \mathbf{m}\mu}^q \mathbf{E}_{\mathbf{m}\mu \times 1}, {}^T \mathbf{B}_{\mathbf{m}\mu \times 1}^3 \Theta_{\mathbf{m}\mu \times \mathbf{m}\mu}^q \mathbf{E}_{\mathbf{m}\mu \times 1}, t \right) \\
\vartheta_2(\tau^1, \tau^2, \tau^3, \tau^4, t) &= {}^T \mathbf{B}_{\mathbf{m}\mu \times 1}^2 \mathbf{E}_{\mathbf{m}\mu \times 1} - \mathbb{O}_2 \left( {}^T \mathbf{B}_{\mathbf{m}\mu \times 1}^1 \Theta_{\mathbf{m}\mu \times \mathbf{m}\mu}^q \mathbf{E}_{\mathbf{m}\mu \times 1}, \right. \\
&\quad \left. {}^T \mathbf{B}_{\mathbf{m}\mu \times 1}^2 \Theta_{\mathbf{m}\mu \times \mathbf{m}\mu}^q \mathbf{E}_{\mathbf{m}\mu \times 1}, {}^T \mathbf{B}_{\mathbf{m}\mu \times 1}^3 \Theta_{\mathbf{m}\mu \times \mathbf{m}\mu}^q \mathbf{E}_{\mathbf{m}\mu \times 1}, t, {}^T \mathbf{B}_{\mathbf{m}\mu \times 1}^4 \Theta_{\mathbf{m}\mu \times \mathbf{m}\mu}^q \mathbf{E}_{\mathbf{m}\mu \times 1}, t \right) \\
\vartheta_3(\tau^1, \tau^2, \tau^3, \tau^4, t) &= {}^T \mathbf{B}_{\mathbf{m}\mu \times 1}^3 \mathbf{E}_{\mathbf{m}\mu \times 1} - \mathbb{O}_3 \left( {}^T \mathbf{B}_{\mathbf{m}\mu \times 1}^1 \Theta_{\mathbf{m}\mu \times \mathbf{m}\mu}^q \mathbf{E}_{\mathbf{m}\mu \times 1}, \right. \\
&\quad \left. {}^T \mathbf{B}_{\mathbf{m}\mu \times 1}^2 \Theta_{\mathbf{m}\mu \times \mathbf{m}\mu}^q \mathbf{E}_{\mathbf{m}\mu \times 1}, {}^T \mathbf{B}_{\mathbf{m}\mu \times 1}^3 \Theta_{\mathbf{m}\mu \times \mathbf{m}\mu}^q \mathbf{E}_{\mathbf{m}\mu \times 1}, t, {}^T \mathbf{B}_{\mathbf{m}\mu \times 1}^4 \Theta_{\mathbf{m}\mu \times \mathbf{m}\mu}^q \mathbf{E}_{\mathbf{m}\mu \times 1}, t \right) \\
\vartheta_4(\tau^1, \tau^2, \tau^3, \tau^4, t) &= {}^T \mathbf{B}_{\mathbf{m}\mu \times 1}^3 \mathbf{E}_{\mathbf{m}\mu \times 1} - \mathbb{O}_3 \left( {}^T \mathbf{B}_{\mathbf{m}\mu \times 1}^1 \Theta_{\mathbf{m}\mu \times \mathbf{m}\mu}^q \mathbf{E}_{\mathbf{m}\mu \times 1}, \right. \\
&\quad \left. {}^T \mathbf{B}_{\mathbf{m}\mu \times 1}^2 \Theta_{\mathbf{m}\mu \times \mathbf{m}\mu}^q \mathbf{E}_{\mathbf{m}\mu \times 1}, {}^T \mathbf{B}_{\mathbf{m}\mu \times 1}^3 \Theta_{\mathbf{m}\mu \times \mathbf{m}\mu}^q \mathbf{E}_{\mathbf{m}\mu \times 1}, t, {}^T \mathbf{B}_{\mathbf{m}\mu \times 1}^4 \Theta_{\mathbf{m}\mu \times \mathbf{m}\mu}^q \mathbf{E}_{\mathbf{m}\mu \times 1}, t \right)
\end{aligned} \tag{2.17}$$

where

$$\begin{aligned}
\tau^1 &= \phi_{1,0}^1, \dots, \phi_{1,\mu-1}^1, \dots, \phi_{\mathbf{m},0}^1, \dots, \phi_{\mathbf{m},\mu-1}^1 \\
\tau^2 &= \phi_{1,0}^2, \dots, \phi_{1,\mu-1}^2, \dots, \phi_{\mathbf{m},0}^2, \dots, \phi_{\mathbf{m},\mu-1}^2 \\
\tau^3 &= \phi_{1,0}^3, \dots, \phi_{1,\mu-1}^3, \dots, \phi_{\mathbf{m},0}^3, \dots, \phi_{\mathbf{m},\mu-1}^3 \\
\tau^4 &= \phi_{1,0}^4, \dots, \phi_{1,\mu-1}^4, \dots, \phi_{\mathbf{m},0}^4, \dots, \phi_{\mathbf{m},\mu-1}^4
\end{aligned}$$

and the terms  $\phi_{\cdot, \cdot}^j$  are the components of  ${}^T \mathbf{C}_{\cdot \times \cdot}^j$ .

Assuming that

$$\begin{aligned}
\vartheta_1(\tau^1, \tau^2, \tau^3, \tau^4, t_{l,j}) &= 0 \\
\vartheta_2(\tau^1, \tau^2, \tau^3, \tau^4, t_{l,j}) &= 0 \\
\vartheta_3(\tau^1, \tau^2, \tau^3, \tau^4, t_{l,j}) &= 0 \\
\vartheta_4(\tau^1, \tau^2, \tau^3, \tau^4, t_{l,j}) &= 0,
\end{aligned}$$

then, we finally obtain a system of  $4\mathbf{m}\mu$  differential equations with  $4\mathbf{m}\mu$  unknowns reading as

$$\begin{aligned}
&\phi_{1,0}^1, \dots, \phi_{1,\mu-1}^1, \dots, \phi_{\mathbf{m},0}^1, \dots, \phi_{\mathbf{m},\mu-1}^1 \\
&\phi_{1,0}^2, \dots, \phi_{1,\mu-1}^2, \dots, \phi_{\mathbf{m},0}^2, \dots, \phi_{\mathbf{m},\mu-1}^2 \\
&\phi_{1,0}^3, \dots, \phi_{1,\mu-1}^3, \dots, \phi_{\mathbf{m},0}^3, \dots, \phi_{\mathbf{m},\mu-1}^3 \\
&\phi_{1,0}^4, \dots, \phi_{1,\mu-1}^4, \dots, \phi_{\mathbf{m},0}^4, \dots, \phi_{\mathbf{m},\mu-1}^4.
\end{aligned}$$

Here, the terms

$$t_{l,j} = \frac{2^\mu i - 1}{2\mu} + l - j - 1, \quad l = 1, 2, \dots, \mathbf{m}; \quad j = 1, 2, \dots, \mu$$

are referred to as the  $\mathbf{m}\mu$  collocation points necessary to successfully preform the approximation process. At this level, we ultimately solve the problem for these unknowns and substitute then into (2.16) to get the numerical solution taking the form

$$\boldsymbol{\eta}(t) = (x_\mu(t), y_\mu(t), z_\mu(t), u_\mu(t))$$

### 3. Numerical representations and interpretations

We proceed now with some numerical simulations using the implementation of the scheme described in the section here above. Using the initial conditions  $\bar{x} = 0$ ,  $\bar{y} = 2$ ,  $\bar{z} = 1$ ,  $\bar{u} = -2$ , we perform in the  $yz$ -plan, numerical representations of the system (2.6)-(2.7), depicting second class types of attractors in the form  $n \times m$ -wings as shown in Fig. 5 to Fig. 10 and having  $n + m$  number of wings. In Fig. 5 where  $q = 1$ ,  $\mathbf{G}(z) = 0$ , the  $4 \times 2$ -wing attractor is similar to the one represented in Fig. 1. Hence, it is also a second class hyperchaotic system with a mirror symmetrical structure. Here, we have used the constant parameter values  $\mathbf{T} = 1$ ,  $\mathbf{M} = 0$ ,  $\rho = 17.9$ ,  $\rho_1 = 1.7$ ,  $\alpha = 18$ . Using (1.4) we obtain  $A_0 = 17.9$ ,  $A_1 = 10.59$ ,  $\tilde{A}_1 = 1.0056$ . The same scenario is observed in Fig. 6 and Fig. 7 with the respective orders  $q = 0.85$  and  $q = 0.70$  where the mirror symmetrical design appears to vary with the parameter  $q$ . The lower and upper parts of the  $4 \times 2$ -wing hyperchaotic attractor are shown to be moving away from the mirror symmetrical junction due to impact of the fractal-fractional operator (2.3) with order  $q$ .

For  $q = 1$ ,  $\mathbf{T} = 7$ ,  $\mathbf{M} = 1$  and taking  $\mathbf{G}(z) \neq 0$  so that  $\Phi = 1.05$ ,  $\tilde{z} = -2.5$ ,  $z_1 = 4$  and then

$$\mathbf{G}(z) = \Phi(1 + \text{sgn}(\text{sgn}(z - \tilde{z}) \times (z - \tilde{z}) - (z_1 - \tilde{z}))),$$

we have in Fig. 8 a  $16 \times 4$ -wing attractor that is similar to the one shown in Fig. 3 and which is also a second class hyperchaotic system with a mirror symmetrical structure. Such a structure extends to Fig. 9 and Fig. 10 with the respective orders  $q = 0.85$  and  $q = 0.70$ . The mirror symmetrical design appears again to vary with the parameter  $q$ . The lower and upper parts of the  $16 \times 4$ -wing hyperchaotic attractor move away from the mirror symmetrical junction due to impact of the fractal-fractional operator. The additional constant parameter values used here are  $\rho = 17.9$ ,  $\rho_1 = 1.7$ ,  $\rho_2 = 1.45$ ,  $\rho_3 = 1$ ,  $\rho_4 = 0.8$ ,  $\rho_5 = 0.65$ ,  $\rho_6 = 0.57$ ,  $\rho_7 = 0.55$ ,  $\alpha = 18$ ,  $A_0 = 17.9$ ,  $A_1 = 10.59$ ,  $A_2 = 12.41$ ,  $A_3 = 18$ ,  $A_4 = 22.5$ ,  $A_5 = 27.69$ ,  $A_6 = 31.58$ ,  $A_7 = 32.73$ ,  $\tilde{A}_1 = 1.0056$ ,  $\tilde{A}_2 = 1.5084$ ,  $\tilde{A}_3 = 2.0112$ ,  $\tilde{A}_4 = 2.514$ ,  $\tilde{A}_5 = 3.0168$ ,  $\tilde{A}_6 = 3.5196$ ,  $\tilde{A}_7 = 4.0223$ .

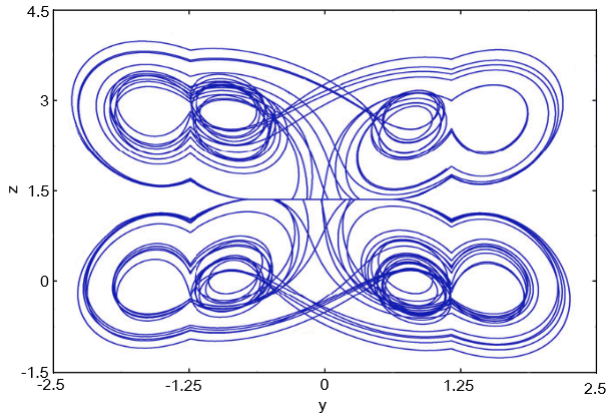


FIGURE 5. Numerical representation of the initial value problem (2.6)-(2.7) with  $q = 1$ , depicting a second class of hyperchaotic attractor (with a mirror junction) of type  $4 \times 2$ -wings in the plan  $yz$ , when  $\mathbf{M} = 0$ ,  $\mathbf{G}(z) = 0$ . The initial conditions used are  $\bar{x} = 0$ ,  $\bar{y} = 2$ ,  $\bar{z} = 1$ ,  $\bar{u} = -2$ . The parameter values used read as  $\mathbf{T} = 1$ ,  $\rho = 17.9$ ,  $\rho_1 = 1.7$ ,  $\rho_2 = 1.45$ ,  $\alpha = 18$  and then,  $A_0 = 17.9$ ,  $A_1 = 10.59$ ,  $A_2 = 12.41$ ,  $\tilde{A}_1 = 1.0056$ ,  $\tilde{A}_2 = 1.5084$ . This attractor is similar to the one represented in Fig. 1

\*

#### 4. Conclusion

We have used in this paper a simple method, consisting on the combination of the fractal and fractional operator with Lü system to generate second class hyperchaotic attractors with many wings divided into rows and columns. This combination has resulted in a modified initial value problem, that we solved numerically. After solving, we have implemented the proposed scheme to perform some numerical representations showing the second class types of attractors in the form  $n \times m$ -wings that appeared to be hyperchaotic and exhibited a mirror symmetrical structure. The graphical simulations have also shown that the lower and upper parts of the second class hyperchaotic attractors are moving away from the mirror symmetrical junction due to the parameter's impact of the fractal-fractional operator. The results obtained in this study show an alternative way of generating second class hyperchaotic attractors without using circuit design and implementation. The knowledge conveyed by this research improves the preceding ones with the generation of the second class hyperchaotic attractor using the fractal and fractional model. Lastly, the moving observation on the attractor's lower and upper parts shows how important the parameters are in changing the dynamical system.

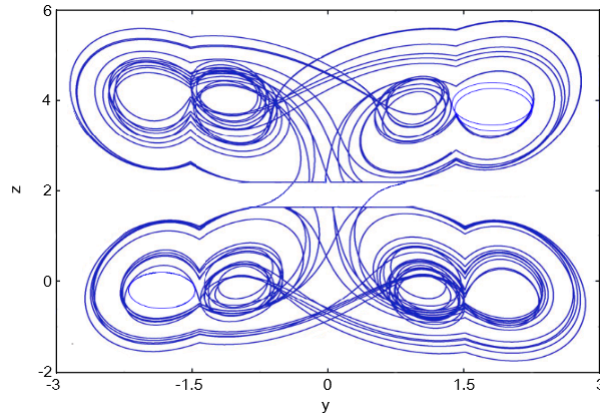


FIGURE 6. Numerical representation of the initial value problem (2.6)-(2.7) with  $q = 0.85$ , depicting a second class of hyperchaotic attractor (with a mirror junction) of type  $4 \times 2$ -wings in the plan  $yz$ , when  $\mathbf{M} = 0$ ,  $\mathbf{G}(z) = 0$ . The initial conditions used are  $\bar{x} = 0$ ,  $\bar{y} = 2$ ,  $\bar{z} = 1$ ,  $\bar{u} = -2$ . The parameter values used read as  $\mathbf{T} = 1$ ,  $\rho = 17.9$ ,  $\rho_1 = 1.7$ ,  $\rho_2 = 1.45$   $\alpha = 18$  and then,  $A_0 = 17.9$ ,  $A_1 = 10.59$ ,  $A_2 = 12.41$ ,  $\bar{A}_1 = 1.0056$ ,  $\bar{A}_2 = 1.5084$ . In this representation, the mirror symmetrical design appears to vary with the parameter  $q$  and the lower and upper parts are shown to be moving away from the mirror symmetrical junction.

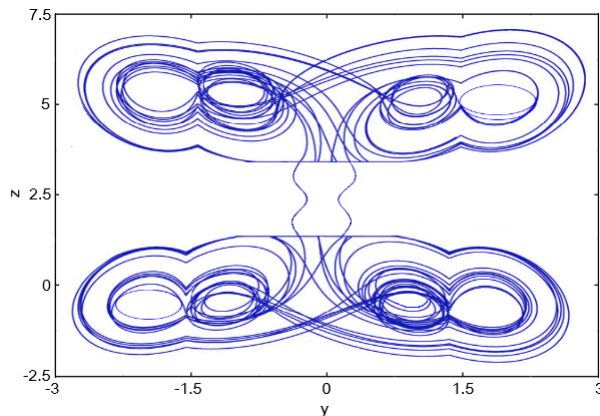


FIGURE 7. Numerical representation of the initial value problem (2.6)-(2.7) with  $q = 0.70$ , depicting a second class of hyperchaotic attractor (with a mirror junction) of type  $4 \times 2$ -wings in the plan  $yz$ , when  $\mathbf{M} = 0$ ,  $\mathbf{G}(z) = 0$ . The initial conditions used are  $\bar{x} = 0$ ,  $\bar{y} = 2$ ,  $\bar{z} = 1$ ,  $\bar{u} = -2$ . The parameter values used read as  $\mathbf{T} = 1$ ,  $\rho = 17.9$ ,  $\rho_1 = 1.7$ ,  $\rho_2 = 1.45$   $\alpha = 18$  and then,  $A_0 = 17.9$ ,  $A_1 = 10.59$ ,  $A_2 = 12.41$ ,  $\bar{A}_1 = 1.0056$ ,  $\bar{A}_2 = 1.5084$ . In this representation, the mirror symmetrical design appears to vary with the parameter  $q$  and the lower and upper parts are shown to be moving further away from the mirror symmetrical junction.

\*

## References

- [1] A. Ahmadova, I. T. Huseynov and N. I. Mahmudov, Controllability of fractional stochastic delay dynamical systems, *arXiv preprint arXiv:2009.10654* (2020).

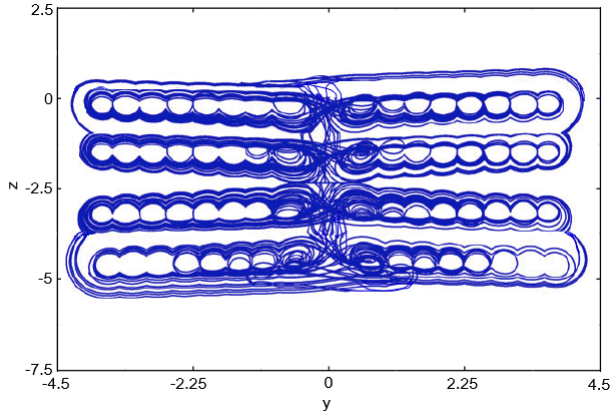


FIGURE 8. Numerical representation of the initial value problem (2.6)-(2.7) with  $q = 1$ , depicting a second class of hyperchaotic attractor (with a mirror junction) of type  $16 \times 4$ -wings in the plan  $yz$ , when  $\mathbf{M} = 1$ , and taking  $\mathbf{G}(z) \neq 0$  with  $\mathbf{G}(z) = \Phi(1 + \text{sgn}(\text{sgn}(z - \bar{z}) \times (z - \bar{z}) - (z_1 - \bar{z})))$  and for  $\mathbf{T} = 7$ , so that  $\Phi = 1.05$ ,  $\bar{z} = -2.5$ ,  $z_1 = 4$ . The initial conditions used are  $\bar{x} = 0$ ,  $\bar{y} = 2$ ,  $\bar{z} = 1$ ,  $\bar{u} = -2$ . The other parameter values used are  $\rho = 17.9$ ,  $\rho_1 = 1.7$ ,  $\rho_2 = 1.45$ ,  $\rho_3 = 1$ ,  $\rho_4 = 0.8$ ,  $\rho_5 = 0.65$ ,  $\rho_6 = 0.57$ ,  $\rho_7 = 0.55$ ,  $\alpha = 18$ ,  $A_0 = 17.9$ ,  $A_1 = 10.59$ ,  $A_2 = 12.41$ ,  $A_3 = 18$ ,  $A_4 = 22.5$ ,  $A_5 = 27.69$ ,  $A_6 = 31.58$ ,  $A_7 = 32.73$ ,  $\tilde{A}_1 = 1.0056$ ,  $\tilde{A}_2 = 1.5084$ ,  $\tilde{A}_3 = 2.0112$ ,  $\tilde{A}_4 = 2.514$ ,  $\tilde{A}_5 = 3.0168$ ,  $\tilde{A}_6 = 3.5196$ ,  $\tilde{A}_7 = 4.0223$ . This attractor is similar to the one represented in Fig. 3.

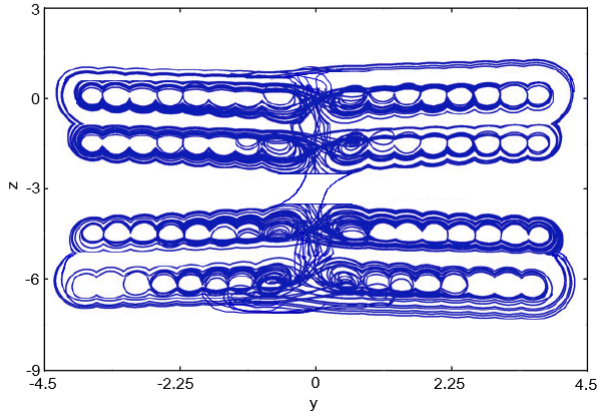


FIGURE 9. Numerical representation of the initial value problem (2.6)-(2.7) with  $q = 0.85$ , depicting a second class of hyperchaotic attractor (with a mirror junction) of type  $16 \times 4$ -wings in the plan  $yz$ , when  $\mathbf{M} = 1$ , and taking  $\mathbf{G}(z) \neq 0$  with  $\mathbf{G}(z) = \Phi(1 + \text{sgn}(\text{sgn}(z - \bar{z}) \times (z - \bar{z}) - (z_1 - \bar{z})))$  and for  $\mathbf{T} = 7$ , so that  $\Phi = 1.05$ ,  $\bar{z} = -2.5$ ,  $z_1 = 4$ . The initial conditions used are  $\bar{x} = 0$ ,  $\bar{y} = 2$ ,  $\bar{z} = 1$ ,  $\bar{u} = -2$ . The other parameter values used are  $\rho = 17.9$ ,  $\rho_1 = 1.7$ ,  $\rho_2 = 1.45$ ,  $\rho_3 = 1$ ,  $\rho_4 = 0.8$ ,  $\rho_5 = 0.65$ ,  $\rho_6 = 0.57$ ,  $\rho_7 = 0.55$ ,  $\alpha = 18$ ,  $A_0 = 17.9$ ,  $A_1 = 10.59$ ,  $A_2 = 12.41$ ,  $A_3 = 18$ ,  $A_4 = 22.5$ ,  $A_5 = 27.69$ ,  $A_6 = 31.58$ ,  $A_7 = 32.73$ ,  $\tilde{A}_1 = 1.0056$ ,  $\tilde{A}_2 = 1.5084$ ,  $\tilde{A}_3 = 2.0112$ ,  $\tilde{A}_4 = 2.514$ ,  $\tilde{A}_5 = 3.0168$ ,  $\tilde{A}_6 = 3.5196$ ,  $\tilde{A}_7 = 4.0223$ . In this representation, the mirror symmetrical design appears to vary with the parameter  $q$  and the lower and upper parts are shown to be moving away from the mirror symmetrical junction.

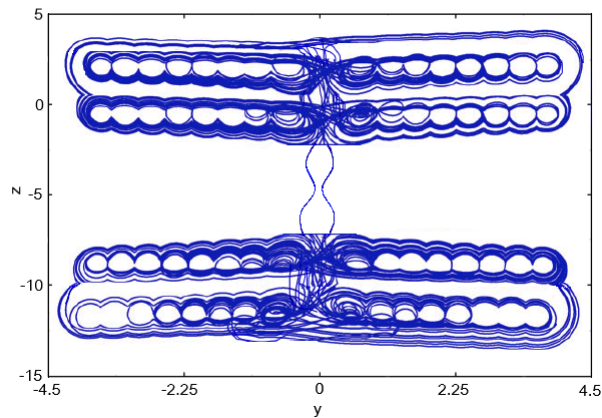


FIGURE 10. Numerical representation of the initial value problem (2.6)-(2.7) with  $q = 0.70$ , depicting a second class of hyperchaotic attractor (with a mirror junction) of type  $16 \times 4$ -wings in the plan  $yz$ , when  $\mathbf{M} = 1$ , and taking  $\mathbf{G}(z) \neq 0$  with  $\mathbf{G}(z) = \Phi(1 + \text{sgn}(\text{sgn}(z - \bar{z}) \times (z - \bar{z}) - (z_1 - \bar{z})))$  and for  $\mathbf{T} = 7$ , so that  $\Phi = 1.05$ ,  $\bar{z} = -2.5$ ,  $z_1 = 4$ . The initial conditions used are  $\bar{x} = 0$ ,  $\bar{y} = 2$ ,  $\bar{z} = 1$ ,  $\bar{u} = -2$ . The other parameter values used are  $\rho = 17.9$ ,  $\rho_1 = 1.7$ ,  $\rho_2 = 1.45$ ,  $\rho_3 = 1$ ,  $\rho_4 = 0.8$ ,  $\rho_5 = 0.65$ ,  $\rho_6 = 0.57$ ,  $\rho_7 = 0.55$ ,  $\alpha = 18$ ,  $A_0 = 17.9$ ,  $A_1 = 10.59$ ,  $A_2 = 12.41$ ,  $A_3 = 18$ ,  $A_4 = 22.5$ ,  $A_5 = 27.69$ ,  $A_6 = 31.58$ ,  $A_7 = 32.73$ ,  $\tilde{A}_1 = 1.0056$ ,  $\tilde{A}_2 = 1.5084$ ,  $\tilde{A}_3 = 2.0112$ ,  $\tilde{A}_4 = 2.514$ ,  $\tilde{A}_5 = 3.0168$ ,  $\tilde{A}_6 = 3.5196$ ,  $\tilde{A}_7 = 4.0223$ . In this representation, the mirror symmetrical design appears to vary with the parameter  $q$  and the lower and upper parts are shown to be moving further away from the mirror symmetrical junction.

- [2] E. Babolian and A. Shamsavaran, Numerical solution of nonlinear fredholm integral equations of the second kind using haar wavelets, *Journal of Computational and Applied Mathematics* **225**(1) (2009) 87–95.
- [3] S. Banihashemi, H. Jafari and A. Babaei, A stable collocation approach to solve a neutral delay stochastic differential equation of fractional order, *Journal of Computational and Applied Mathematics* **403** (2022) p. 113845.
- [4] E. Bieberich, Recurrent fractal neural networks: a strategy for the exchange of local and global information processing in the brain, *Biosystems* **66**(3) (2002) 145–164.
- [5] S. Caruthers and T. Harris, Effects of pulmonary blood flow on the fractal nature of flow heterogeneity in sheep lungs, *Journal of Applied Physiology* **77**(3) (1994) 1474–1479.
- [6] A. Chen, J. Lu, J. Lü and S. Yu, Generating hyperchaotic liu attractor via state feedback control, *Physica A: Statistical Mechanics and its Applications* **364** (2006) 103–110.
- [7] Z. Chen, Y. Yang and Z. Yuan, A single three-wing or four-wing chaotic attractor generated from a three-dimensional smooth quadratic autonomous system, *Chaos, Solitons & Fractals* **38**(4) (2008) 1187–1196.
- [8] Y. Chen, M. Yi and C. Yu, Error analysis for numerical solution of fractional differential equation by Haar wavelets method, *Journal of Computational Science* **3**(5) (2012) 367–373.
- [9] L. Chua, M. Komuro and T. Matsumoto, The double scroll family, *IEEE transactions on circuits and systems* **33**(11) (1986) 1072–1118.
- [10] E. F. Doungmo Goufo, The proto-lorenz system in its chaotic fractional and fractal structure, *International Journal of Bifurcation and Chaos* **30**(12) (2020) p. 2050180.

- [11] E. F. Doungmo Goufo, Mathematical analysis of peculiar behavior by chaotic, fractional and strange multiwing attractors, *International Journal of Bifurcation and Chaos* **28**(10) (2018) p. 1850125.
- [12] E. F. D. Goufo, On the fractal dynamics for higher order traveling waves, *Chaos, Solitons & Fractals* **148** (2021) p. 111059.
- [13] E. F. D. Goufo, Fractal and fractional dynamics for a 3d autonomous and two-wing smooth chaotic system, *Alexandria Engineering Journal* (2020).
- [14] E. F. D. Goufo and Y. Khan, A new auto-replication in systems of attractors with two and three merged basins of attraction via control, *Communications in Nonlinear Science and Numerical Simulation* (2021) p. 105709.
- [15] S. B. Heydarova, On fredholm property of a boundary value problem for third order operator-differential equations, *Proceedings of the Institute of Mathematics and Mechanics* **46**(1) (2020), 159–166.
- [16] S. Hotton and J. Yoshimi, Extending dynamical systems theory to model embodied cognition, *Cognitive Science* **35**(3) (2011) 444–479.
- [17] H. Jafari, K. Goodarzi, M. Khorshidi, V. Parvaneh and Z. Hammouch, Lie symmetry and  $\mu$ -symmetry methods for nonlinear generalized camassa–holm equation, *Advances in Difference Equations* **2021**(1) (2021) 1–12.
- [18] Ü. Lepik and H. Hein, *Haar Wavelets: With Applications* (Springer Science & Business Media, 2014).
- [19] Y. Li, Z. Li, M. Ma and M. Wang, Generation of grid multi-wing chaotic attractors and its application in video secure communication system, *Multimedia Tools and Applications* **79**(39) (2020) 29161–29177.
- [20] E. N. Lorenz, Deterministic nonperiodic flow, *Journal of the atmospheric sciences* **20**(2) (1963) 130–141.
- [21] J. Lü and G. Chen, A new chaotic attractor coined, *International Journal of Bifurcation and Chaos* **12**(03) (2002) 659–661.
- [22] J. Lü and G. Chen, Generating multiscroll chaotic attractors: theories, methods and applications, *International Journal of Bifurcation and Chaos* **16**(04) (2006) 775–858.
- [23] P. Melby, N. Weber and A. Hübler, Dynamics of self-adjusting systems with noise, *Chaos: An Interdisciplinary Journal of Nonlinear Science* **15**(3) (2005) p. 033902.
- [24] C. Ravichandran, K. Jothimani, H. M. Baskonus and N. Valliammal, New results on nondensely characterized integrodifferential equations with fractional order, *The European Physical Journal Plus* **133**(3) (2018) 1–9.
- [25] O. Rossler, An equation for hyperchaos, *Physics Letters A* **71**(2-3) (1979) 155–157.
- [26] H. S. Rzayeva, Global bifurcation of solutions of nonlinear one-dimensional dirac system, *Proceedings of the Institute of Mathematics and Mechanics* **41**(2) (2015), 36–46.
- [27] H. Tajadodi, N. Kadkhoda, H. Jafari and M. Inc, Approximate technique for solving fractional variational problems, *Pramana* **94**(1) (2020) 1–8.
- [28] M. Yalcin, J. Suykens and J. Vandewalle, Experimental confirmation of 3-and 5-scroll attractors from a generalized chua’s circuit, *IEEE Transactions on Circuits and Systems I: Fundamental Theory and Applications* **47**(3) (2000) 425–429.
- [29] S. Yu, W. K. Tang, J. Lü and G. Chen, Generating 2n-wing attractors from lorenz-like systems, *International Journal of Circuit Theory and Applications* **38**(3) (2010) 243–258.
- [30] C. Zhang and S. Yu, On constructing complex grid multi-wing hyperchaotic system: theoretical design and circuit implementation, *International Journal of Circuit Theory and Applications* **41**(3) (2013) 221–237.

*University of South Africa, Florida, 0003, South Africa*

E-mail address: `franckemile2006@yahoo.ca`

Received: March 21, 2022; Revised: July 22, 2022; Accepted: August 7, 2022